

Articles

Synthesis, Structural Characterization, and Theoretical Treatment of an Unusual Organozirconium Hydroxide with the $[\text{Zr}_6(\mu_4\text{-O})(\mu\text{-O})_4(\mu\text{-OH})_8]$ Core[†]

Guangcai Bai, Herbert W. Roesky,* Jiyang Li, Thomas Labahn, Fanica Cimpoesu, and Jörg Magull

Institut für Anorganische Chemie der Universität Göttingen, Tammannstrasse 4, D-37077 Göttingen, Germany

Received February 20, 2003

A novel organozirconium hydroxide, $[(\text{Cp}^*\text{Zr})_6(\mu_4\text{-O})(\mu\text{-O})_4(\mu\text{-OH})_8] \cdot 2(\text{C}_7\text{H}_8)$ (**2**), was prepared by the hydrolysis of Cp^*ZrCl_3 . For the preparation of **2** the reagents KOH and water and the two-phase system ammonia/toluene were used. The crystal structure reveals that **2** is an octahedron comprising Cp^*Zr fragments arranged around an interstitial oxygen atom that preferentially occupies two off-center positions, 0.933(13) Å apart from each other. The six Cp^*Zr fragments are bridged by a total of 12 $\mu\text{-O}$ and $\mu\text{-OH}$ groups. Molecular mechanical and ab initio calculations were carried out in order to analyze the stability and the bonding environment of the off-center structure by comparing to that with the ideal $\mu_6\text{-O}$ arrangement.

Introduction

In recent years the chemistry of derivatized organic polyoxometal clusters has attracted great interest in terms of their catalytic properties and size in the nanometer range and as a modeling system for the reactivities and properties of metal oxides in solution.¹ In general, hydrolysis of zirconium halides leads to zirconium oxides or hydroxides. Representative organozirconium oxides or hydroxides include $[(\text{Cp}_2\text{ZrCl})_2(\mu\text{-O})]_2$,² $\{[\text{CpZr}(\mu\text{-OH})(\text{H}_2\text{O})_3]_2(\text{CF}_3\text{SO}_3)_4\} \cdot \text{THF}$,³ $\{[\text{CpZr}(\mu\text{-OH})_3(\mu_3\text{-O})(\mu\text{-PhCOO})_3]^+[\text{PhCOO}^-] \cdot \text{OEt}_2\}$,⁴ $\{[\text{Cp}^*\text{-ZrCl}(\mu\text{-OH})_3(\mu_3\text{-OH})(\mu_3\text{-O})] \cdot 2\text{THF} (\text{Cp}^* = \text{C}_5\text{Me}_5)\}$,⁵ $\{[\text{Cp}^*\text{ZrCl}(\mu\text{-OH})_3(\mu_3\text{-O})(\mu\text{-Cl})]_6\}$,⁶ $[(\text{Cp}^*\text{ZrCl})_3(\mu\text{-Cl})_4(\mu_3\text{-O})]$, $\{[\text{Cp}^*\text{ZrCl}_2(\mu\text{-OH})(\text{H}_2\text{O})]_2\}$,⁷ and $\{[\text{Cp}_2\text{Zr}(\mu\text{-OH})_3(\mu_3\text{-O})]^+(\text{BPh}_4)^-\}$.⁸ Recently, the organozirconium oxide clusters $\{[(\text{EtMe}_4\text{C}_5\text{Zr})_6(\mu_6\text{-O})(\mu_3\text{-O})_8] \cdot (\text{C}_7\text{H}_8)$ and

$\{[(\text{EtMe}_4\text{C}_5\text{Zr})_6(\mu_6\text{-O})(\mu_3\text{-O})_8] \cdot (\text{C}_9\text{H}_{12})$ have been prepared by the hydrolysis of metal chlorides in a liquid ammonia/toluene two-phase system at low temperatures.⁹ These oxide clusters are soluble analogues of discrete fragments of solid ZrO_2 , in which there are no reactive OH groups that could undergo further reactions and all the oxygen and zirconium atoms are coordinatively saturated.

Polyoxometallic supported transition metal catalysts that can be fully investigated at the atomic level both structurally and mechanistically represent a new development of oxide-supported catalysts.¹⁰ Meanwhile, the interest in studying the nature of the surface containing hydroxyl groups on inorganic oxides has been increased due to the application as solid acid catalysts and (silica, alumina, zeolite, etc.) supported metal catalysts.¹¹ Organopolyoxometal hydroxide clusters and organopolyoxozirconium-supported metal complexes are very rare.

[†] Dedicated to Professor Heinrich Nöth on the occasion of his 75th birthday.

* To whom correspondence should be addressed. E-mail: hroesky@wdg.de.

(1) (a) Klemperer, W. G.; Wall, C. G. *Chem. Rev.* **1998**, *98*, 297–306. (b) Gouzerh, P.; Proust, A. *Chem. Rev.* **1998**, *98*, 77–111. (c) Kickelbick, G.; Schubert, U. *Monatsh. Chem.* **2001**, *132*, 13–30. (d) Bottomley, F. *Polyhedron* **1992**, *11*, 1707–1731. (e) Day, V. W.; Klemperer, W. G. *Science* **1985**, *228*, 533–541.

(2) Clarke, J. F.; Drew, M. G. B. *Acta Crystallogr.* **1974**, *B30*, 2267–2269.

(3) Lasser, W.; Thewalt, U. *J. Organomet. Chem.* **1986**, *311*, 69–77.

(4) Thewalt, U.; Döppert, K.; Lasser, W. *J. Organomet. Chem.* **1986**, *308*, 303–309.

(5) Babcock, L. M.; Day, V. W.; Klemperer, W. G. *J. Chem. Soc., Chem. Commun.* **1988**, 519–520.

(6) Babcock, L. M.; Day, V. W.; Klemperer, W. G. *Inorg. Chem.* **1989**, *28*, 806–810.

(7) Hidalgo, G.; Pellinghelli, M. A.; Royo, P.; Serrano, R.; Tiripicchio, A. *J. Chem. Soc., Chem. Commun.* **1990**, 1118–1120.

(8) Niehues, M.; Erker, G.; Meyer, O.; Fröhlich, R. *Organometallics* **2000**, *19*, 2813–2815.

(9) Bai, G.; Roesky, H. W.; Lobinger, P.; Noltemeyer, M.; Schmidt, H.-G. *Angew. Chem.* **2001**, *113*, 2214–2217; *Angew. Chem., Int. Ed.* **2001**, *40*, 2156–2159.

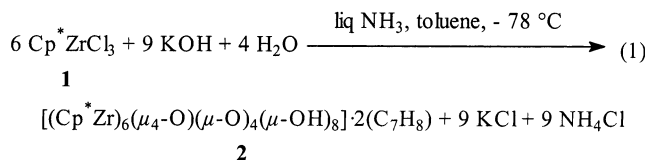
(10) (a) Pohl, M.; Lyon, D. K.; Mizuno, N.; Nomiya, K.; Finke, R. G. *Inorg. Chem.* **1995**, *34*, 1413–1429, and references therein. (b) Day, V. W.; Earley, C. W.; Klemperer, W. G.; Maltbie, D. J. *J. Am. Chem. Soc.* **1985**, *107*, 8261–8262.

(11) (a) Iwasawa, Y. *Tailored Metal Catalysts*; D. Reidel Publishing Company: Dordrecht, The Netherlands, 1986; pp 1–85. (b) Cale, J. D.; Catlow, C. R. A.; Carruthers, J. R. *Chem. Phys. Lett.* **1993**, *216*, 155–161. (c) Jezequel, M.; Dufaud, V.; Ruiz-Garcia, M. J.; Carrillo-Hermosilla, F.; Neugebauer, U.; Nicolai, G. P.; Lefebvre, F.; Bayard, F.; Corker, J.; Fiddy, S.; Evans, J.; Broyer, J.-P.; Malinge, J.; Basset, J.-M. *J. Am. Chem. Soc.* **2001**, *123*, 3520–3540. (d) Park, C.; Keane, M. A. *J. Mol. Catal. A: Chem.* **2001**, *166*(2), 303–322.

Herein, we report the first organozirconium hydroxide cluster that contains eight OH groups that may serve as a precursor model in the construction of functionalized organopolyoxometallic supported catalysts in homogeneous catalysis.

Results and Discussion

Synthesis of 2. The reaction of Cp^*ZrCl_3 (**1**) with KOH containing 10–15% H_2O (1:1.5 molar ratio) in liquid ammonia and toluene at -78°C results in the complete removal of chloride and the formation of an organozirconium hydroxide, $[(\text{Cp}^*\text{Zr})_6(\mu_4\text{-O})(\mu\text{-O})_4(\mu\text{-OH})_8]\cdot 2(\text{C}_7\text{H}_8)$ (**2**; eq 1). It has been generally observed



that the complete hydrolysis of zirconium chlorides leading to zirconium oxides or hydroxides without an appreciable amount of chloride is difficult to achieve.^{6,12} The liquid ammonia affords the complete removal of the chloride and the formation of **2**. It is assumed that the formation of **2** proceeds via zirconium water adduct and hydroxide intermediates,⁹ which after inter- or intramolecular elimination of hydrochloride as NH_4Cl and KCl are converted to **2**. We were unable to isolate **2** from the reaction of **1** with H_2O in liquid ammonia and toluene. Obviously, the KOH, H_2O , and the liquid ammonia system completely cleaves the $\text{Zr}-\text{Cl}$ bonds and converts the resulting ZrOH and $\text{Zr}(\text{OH})_2$ to ZrOZr and $\text{Zr}(\mu\text{-OH})\text{Zr}$ species. Furthermore, the two-phase system (ammonia/toluene) increases the solubility of the organic and inorganic components, so that the reaction preferentially proceeds at the interface.

Compound **2** is a colorless crystalline solid with unusual thermal stability. The melting point of **2** exceeds 410°C . Under an inert atmosphere no decomposition is observed for **2** during the recrystallization (in toluene) and in the solid state or in solution (toluene) over a period of one year. The IR spectrum of **2** shows a broad absorption at 3689 cm^{-1} , assignable to the $\text{O}-\text{H}$ stretching frequency. In the EI mass spectrum of **2**, the most intense peak appears at m/z 119 $[\text{Cp}^* - \text{CH}_4]^+$, and the signal at 1367 (56%) is assigned to the $[\text{M} - 2\text{C}_7\text{H}_8 - \text{Cp}^* - 4\text{H}_2\text{O}]^+$ fragment. The signals at 1646 (2%) and 1512 (18%), assignable to the $[\text{M} - \text{C}_7\text{H}_8 - \text{H}_2\text{O}]^+$ and $[\text{M} - \text{C}_7\text{H}_8 - \text{Cp}^* - \text{H}_2\text{O} - \text{H}]^+$ fragments, indicate that one molecule of toluene is captured by the cluster in the gas phase under EI-MS conditions. The ^1H NMR spectrum of **2** exhibits a single resonance (δ 2.05 ppm) for the Cp^* protons, which can be interpreted as six equivalent Cp^* groups of **2** in solution. No resonance corresponding to the protons of the OH groups on zirconium is observed in the solution ^1H NMR spectrum of **2**. The elemental analysis of **2** shows that the composition of C, H, and Zr is consistent with the formula $[(\text{Cp}^*\text{Zr})_6(\mu_4\text{-O})(\mu\text{-O})_4(\mu\text{-OH})_8]\cdot 2(\text{C}_7\text{H}_8)$.

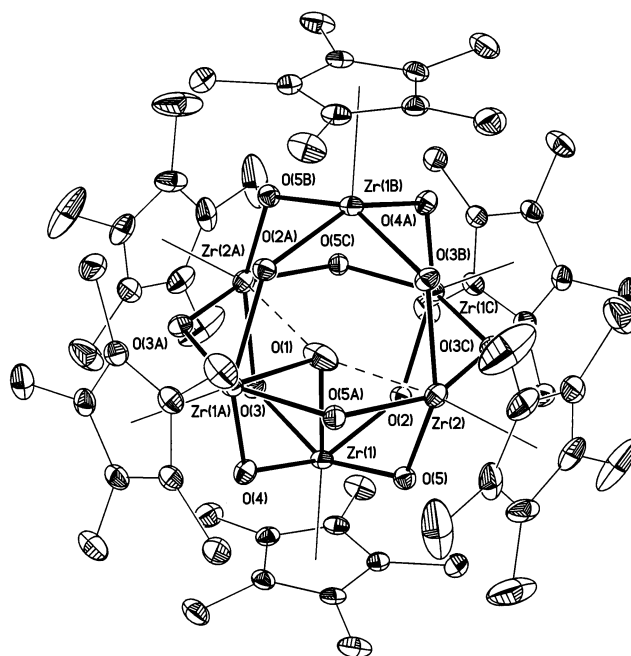


Figure 1. Molecular structure of $[(\text{Cp}^*\text{Zr})_6(\mu_4\text{-O})(\mu\text{-O})_4(\mu\text{-OH})_8]\cdot 2(\text{C}_7\text{H}_8)$ (**2**) in the crystal (50% probability ellipsoids; two toluene molecules and H atoms bonded to C and O are omitted for clarity).

Molecular Structure of 2. Single crystals of **2**, suitable for X-ray structural analysis, were obtained from toluene by keeping the reaction mixture at room temperature for one month. The molecular structure of **2** is shown in Figure 1. With four $[(\text{Cp}^*\text{Zr})_6(\mu_4\text{-O})(\mu\text{-O})_4(\mu\text{-OH})_8]\cdot 2(\text{C}_7\text{H}_8)$ in the unit cell **2** crystallizes in the monoclinic space group $C2/m$. The molecular structure of **2** consists of an octahedron with Cp^*Zr fragments arranged around an interstitial oxygen atom that preferentially occupies two positions, $0.933(13)\text{ \AA}$ apart from each other. The angles between adjacent zirconium atoms are either 60° or 89° . Twelve edges of the octahedron are bridged by each oxygen, resulting in eight six-membered Zr_3O_3 rings with chair conformation. The average $\text{O}-\text{Zr}-\text{O}$ and $\text{Zr}-\text{O}-\text{Zr}$ angles in the Zr_3O_3 rings are 86.11° ($82.76(6)-88.94(10)^\circ$) and 120.56° ($118.70(14)-122.78(12)^\circ$). The coordination sphere of each zirconium is completed by the Cp^* ligand. The $\text{Zr}-(\mu\text{-O})$ or $\text{Zr}-(\mu\text{-OH})$ bond lengths ($2.072(2)-2.171(2)\text{ \AA}$, av 2.106 \AA) are similar to those in $[(\text{Cp}^*\text{ZrCl})(\mu\text{-OH})_3(\mu_3\text{-OH})(\mu_3\text{-O})]\cdot 2\text{THF}$ ($\text{Zr}-(\mu\text{-OH})$ $2.160(2)\text{ \AA}$).⁵ Moreover the $\text{Zr}-(\mu\text{-O})$ and $\text{Zr}-(\mu\text{-OH})$ bond lengths are longer than those in $[(\text{Cp}_2\text{ZrCl})_2(\mu\text{-O})]$ ($\text{Zr}-(\mu\text{-O})$ $1.945(3)\text{ \AA}$)² and $[(\text{Cp}_2\text{Zr}(\mu\text{-O}))_3]$ ($\text{Zr}-(\mu\text{-O})$ $1.959(3)\text{ \AA}$)¹³ and are comparable with the $\text{Zr}-(\mu_3\text{-O})$ bond distances in $[(\text{EtMe}_4\text{C}_5\text{Zr})_6(\mu_6\text{-O})(\mu_3\text{-O})_8]\cdot (\text{C}_7\text{H}_8)$ ($2.136(2)-2.169(2)\text{ \AA}$, av 2.156 \AA).⁹ In general, the $\text{M}-(\mu\text{-OH})$ bond length ($\text{M} = \text{metal}$) is longer than that of $\text{M}-(\mu\text{-O})$. The X-ray diffraction study of **2** failed to distinguish between $\mu\text{-O}$ and $\mu\text{-OH}$ groups. The eight hydrogen atoms of OH groups should be distributed over 12 edging positions or bridged between the adjacent $\mu\text{-O}$ groups, but the occupancy is difficult to confirm. The $\text{Zr}\cdots\text{Zr}$ distances ($3.564(1)-3.608(1)\text{ \AA}$, av 3.586 \AA) are significantly longer than those in $[(\text{EtMe}_4\text{C}_5\text{Zr})_6(\mu_6\text{-O})(\mu_3\text{-O})_8]\cdot (\text{C}_7\text{H}_8)$

(12) Henderson, A. W.; Higbie, K. B. *J. Am. Chem. Soc.* **1954**, *76*, 5878–5879.

(13) Fachinetti, G.; Floriani, C.; Chiesi-Villa, A.; Guastini, C. *J. Am. Chem. Soc.* **1979**, *101*, 1767–1775.

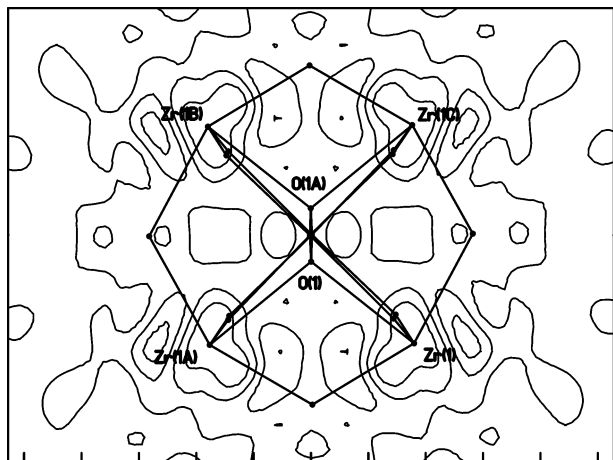


Figure 2. Residual electron density map of $[(\text{Cp}^*\text{Zr})_6(\mu_4\text{-O})(\mu\text{-O})_4(\mu\text{-OH})_8]\cdot 2(\text{C}_7\text{H}_8)$ (**2**).

(3.1542(9)–3.1709(11) Å, av 3.1635 Å) and those exhibited by the amidoimidonitrido zirconium complex¹³ and the zirconium halide clusters.¹⁴

The Zr(1)–O(1) (2.292(4) Å) and Zr(1A)–O(1) (2.292(4) Å) bond lengths are similar to those in $[(\text{EtMe}_4\text{C}_5\text{-Zr})_6(\mu_6\text{-O})(\mu_3\text{-O})_8]\cdot(\text{C}_7\text{H}_8)$ (Zr–($\mu_6\text{-O}$) 2.231(2)–2.247(2) Å, av 2.241 Å). The longer distances of Zr(2)–O(1) (2.610(10) Å) and Zr(2A)–O(1) (2.554(10) Å) suggest that there are weak bonding interactions between these atoms. The long Zr(1B)–O(1) (2.966 Å) and Zr(1C)–O(1) (2.966 Å) contacts also indicate the very weak interactions between them. It is assumed that the interstitial atoms generally exert a stabilizing influence on a metal cluster by acting as an “atomic glue”. While the small size of the oxygen makes it difficult to fit into the big size of the octahedral skeleton of **2** (the average distance of the octahedron center to zirconium atoms is 2.586 Å, which is distinctly longer than that of $[(\text{EtMe}_4\text{C}_5\text{-Zr})_6(\mu_6\text{-O})(\mu_3\text{-O})_8]\cdot(\text{C}_7\text{H}_8)$ (Zr–($\mu_6\text{-O}$) 2.241 Å)), only two strong and two weaker bonds are formed. Residual electron density for the interstitial oxygen atom was resolved in an electron density difference map. As shown in Figure 2, the off-center positions become visible in the $F_o - F_c$ map, whereas no residual electron density at the center is found.

Theoretical Treatment of the $[\text{Zr}_6(\mu_4\text{-O})(\mu\text{-O})_{12}]$ and $[\text{Zr}_6(\mu_6\text{-O})(\mu\text{-O})_{12}]$ Cores. It is interesting to observe from the X-ray diffraction study of **2** that the electron density of the interstitial oxygen atom is mainly distributed over O(1) and O(1A) atoms, and no residual electron density was found at the central position (Figure 2). Molecular mechanical simulation was done in order to investigate the structural character of the interstitial oxygen atom. Models A and B (Figure 3), based on the experimental data, were built to simulate the observed and hypothetical interstitial oxygen positions of O(1) and Oc (center of **2**). Model A, with the same structure as **2** (not including the eight protons), contains the off-center arrangement $[\text{Zr}_6(\mu_4\text{-O})(\mu\text{-O})_{12}]$, and model B has the ideal $\mu_6\text{-O}$ core $[\text{Zr}_6(\mu_6\text{-O})(\mu\text{-O})_{12}]$ (Zr–($\mu_6\text{-O}$), 2.539–2.644 Å, av 2.608 Å). Molecular

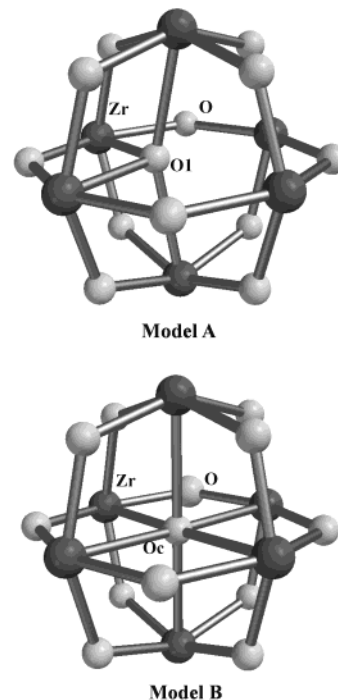


Figure 3. Cores of two simulated models. Model A: $[(\text{Cp}^*\text{Zr})_6(\mu_4\text{-O})(\mu\text{-O})_{12}]^{-8}$, with the same structure as **2** (the eight protons not included). Model B: $[(\text{Cp}^*\text{Zr})_6(\mu_6\text{-O})(\mu\text{-O})_{12}]^{-8}$, $\mu_6\text{-O}$ at the central position Oc.

mechanical calculations, based on the MMFF94 force field,¹⁵ were used to compare the energies of models A and B in exactly similar experimental environments and were found to be impossible by RHF or DFT calculations due to the eight indefinite protons. The calculated results show that the single-point energy of model A (1876.94 kcal/mol) is smaller than that of model B (2986.59 kcal/mol). This finding indicates that the structure of **2**, with the off-center oxygen atom at the O(1) position, is more favorable than that with the ideal $\mu_6\text{-O}$ core, in agreement with the experimental results.

Ab initio calculations¹⁶ were carried out to optimize and analyze the bonding environment of the frozen off-center structure by comparison to that of the ideal $\mu_6\text{-O}$ core. Thus, taking the experimental structure of **2**, the RHF and DFT calculations (by B3LY) yield the following bond orders (for DFT, noted in parentheses): 0.362 (0.393) for the shorter two contacts, 0.342 (0.373) and 0.327 (0.368) for the intermediate ones, and 0.193 (0.256) for the two longest Zr...O interactions. For the structure with the oxygen at the center of inversion, the bond orders are dichotomized in two 0.324 (0.352) and four 0.294(0.346) values. The total bond orders of the center core (1.821 (2.089)) and the off-center one (1.778

(15) (a) Molecular mechanics calculations were performed in the Spartan'02 software: Halgren, T. A. *J. Comput. Chem.* **1996**, *17*, 490–519. (b) For simulating the exactly experimental environment, no geometry optimization of models A and B was performed.

(16) (a) The RHF (restricted Hartree–Fock) and B3LYP-DFT (density functional theory) calculations were performed with 3-21G basis sets using the GAMESS package: Schmidt, M. W.; Baldridge, K. K.; Boatz, J. A.; Elbert, S. T.; Gordon, M. S.; Jensen, J. H.; Koseki, S.; Matsunaga, N.; Nguyen, K. A.; Su, S. J.; Windus, T. L.; Dupuis, M.; Montgomery, J. A. *J. Comput. Chem.* **1993**, *14*, 1347–1363. (b) For the sake of simplicity, the terminal ligands were taken as Cp. (c) We assign the hydrogen center having a nuclear charge $Z^* = 2/3$. In this manner, one conventionally simulates the smearing out of 8 protons on the 12 equivalent edges, while the electron count is the same as in the $(\text{CpZr})_6\text{O}(\mu\text{-O})_4(\mu\text{-OH})_8$ species.

(14) (a) Ziebarth, R. P.; Corbett, J. D. *J. Am. Chem. Soc.* **1987**, *109*, 4844–4850. (b) Smith, J. D.; Corbett, J. D. *J. Am. Chem. Soc.* **1985**, *107*, 5704–5711. (c) Imoto, H.; Corbett, J. D.; Cisar, A. *Inorg. Chem.* **1981**, *20*, 145–151. (d) Ziebarth, R. P.; Corbett, J. D. *J. Solid State Chem.* **1989**, *80*, 56–67.

(2.039) are comparable. At the RHF level, the μ_6 -O core is a little more stable (13 kcal) than that of the off-centered one, while the DFT calculation reveals practically almost equal energies (the distorted one becomes more stable by 0.75 kcal). From this viewpoint, compounds with the $[\text{Zr}_6(\mu_6\text{-O})(\mu\text{-O})_{12}]$ core structure should exist under certain conditions.

The vibrational analysis of the symmetric structure (optimized under RHF) shows many low-frequency modes including the deformation of the Zr_6O moiety. The cumulative results allow us to conclude that the inner μ_6 -O atom possesses a floppy nature, and the total bonding effects are comparable in both the center and the off-center positions. This result explains qualitatively the experimentally observed disorder. The comparison of RHF and DFT results suggests that the fine effects of electron correlation (included in the last method) contribute to the distortion tendency. It is important to note that these results are obtained under the imposed approximation and simulation of the disorder of protons as a symmetrical averaged field.^{16b} Within this model, the geometry optimization leads to a $[\text{Zr}_6(\mu_6\text{-O})(\mu\text{-O})_{12}]$ skeleton with an almost octahedral structure whose computed $\text{Zr}-(\mu\text{-O})$ (2.07 Å) value is in agreement with the experimental one (2.07–2.17 Å).

The account of statistical or dynamical disorder of the protons is prohibitive for a direct contribution in the calculation. However, it is likely that slow proton dynamics is also a factor favoring the frozen cluster distortion. With respect to the octahedral geometry, the off-center deformation within the octahedral pattern has the shape of a pseudo Jahn–Teller distortion.¹⁷

The particular structural effects in **2** are similar to those determined for the solid phase of various perovskites (Ti, Zr, or Hf)¹⁸ and also similar to those phenomenon of negative thermal expansion in certain mixed oxides of zirconium.¹⁹

OH Functional Groups of 2. The OH groups are the most important functional groups of solid support for the immobilization of catalytically active metal complexes and also for solid acid catalysts. It has been demonstrated that the gradient of the electrostatic potential at the proton correlates with the O–H stretching frequency.²⁰ Therefore, the stretching mode of the O–H group is a qualitative indicator for the acidity of a proton.

Due to the Lewis Zr(IV) centers, the OH groups of **2** are expected to be Brønsted acidic. The absorption of the hydroxyl groups in the IR spectrum of **2** (3689 cm^{-1}) is higher than those found in the Brønsted acids SAPO-34 (3600–3625 cm^{-1})²¹ and zeolite Chabazite (3603 cm^{-1})²² and significantly higher than those found in the other zirconium hydroxides, such as $[\text{Cp}_2\text{Zr}(\text{OCOFC}_3)-$

$(\mu\text{-OH})_2$ (3640 cm^{-1}),²³ $[\{(\text{Cp}_2\text{Zr})_3(\mu\text{-OH})_3(\mu_3\text{-O})\}^+(\text{BPh}_4)^-]$ (3567 cm^{-1}),⁸ $[\{\text{Cp}^*\text{ZrCl}_2(\mu\text{-OH})(\text{H}_2\text{O})\}_2]$ (3533 cm^{-1}),⁷ and $[\{(\text{Cp}^*\text{ZrCl})(\mu\text{-OH})\}_3(\mu_3\text{-OH})(\mu_3\text{-O})]\cdot 2\text{THF}$ (3655, 3618, 3520, and 3425 cm^{-1}).⁵ However, the ¹H NMR spectral investigations failed to demonstrate the Brønsted acidity of **2** in both solution and solid state.

Summary

In this part of the study, a new method for the preparation of organozirconium hydroxides, such as **2**, by hydrolysis of an organozirconium chloride at low temperature has been demonstrated. The formation of **2** presumably proceeds via the zirconium/water adduct and hydroxide intermediates. The KOH, H₂O, and the two-phase system (NH₃/toluene) are important for the formation of **2**. The central inorganic core of **2** (overlooking the disordering of the interstitial oxygen atom) can be regarded as a derivative of $[\{(\text{EtMe}_4\text{C}_5\text{Zr})_6(\mu_6\text{-O})(\mu_3\text{-O})_8\}(\text{C}_7\text{H}_8)]$, in which the $\mu\text{-O}$ and $\mu\text{-OH}$ species replace the $\mu_3\text{-O}$ units. The long $\text{Zr}\cdots\text{Zr}$ distances in **2**, which result from the 24 bridging $\text{Zr}-(\mu\text{-O})$ bonds, led to the deviation of the interstitial oxygen atom from the center of the octahedral skeleton with the formation of only two strong and two weaker $\text{Zr}-\text{O}$ bonds. The compound with the $[\text{Zr}_6(\mu_4\text{-O})(\mu\text{-O})_{12}]$ core is more stable than that with the $[\text{Zr}_6(\mu_6\text{-O})(\mu\text{-O})_{12}]$ skeleton according to the molecular mechanical calculations. Based on two models simulated by the X-ray diffraction data of **2**, the calculations explain why the interstitial oxygen atom of **2** occupies preferentially the two off-center positions. The ab initio calculations indicate that the interstitial oxygen atom possesses a floppy nature and the stability of the $\mu_6\text{-O}$ core is comparable to that of the off-center one. Therefore, it should be possible to prepare a compound with the ideal $\mu_6\text{-O}$ core structure. The O–H stretching frequencies indicate that **2** is a Brønsted acid. The organic ligands and the reactive hydroxide groups on the cluster surface facilitate the solubility of **2** and hence its reactivity in solution. A wide variety of organometallic complexes should react with the Brønsted acidic OH groups of **2**, giving well-characterized and soluble metal clusters. This area of chemistry is still in its infancy, but provides incentives to the development of a new and exciting molecular catalytic approach in a homogeneous system. Further studies using **2** for the preparation of new homo- or heterometallic clusters and their application as homogeneous catalysts are in progress.

Experimental Section

General Remarks. All manipulations were carried out under an atmosphere of purified nitrogen using standard Schlenk techniques. Samples prepared for spectral measurements as well as for reactions were manipulated in a glovebox. Solvent was dried using conventional procedures, distilled under nitrogen, and degassed prior to use. Deuterated NMR solvents were treated with K/Na alloy, distilled, and stored under nitrogen.

The ¹H NMR spectra were recorded on a Bruker AM 20 NMR spectrometer with SiMe₄ as external standard. Mass spectra were recorded on a Finnigan MAT 8230 mass spectrometer using the EI-MS method. The most intensive peak

(17) Maaskant, W. J. A.; Bersuker, I. B. *J. Phys. Condens. Mater.* **1991**, *3*, 37–47.

(18) (a) Bersuker, I. B. *Ferroelectrics* **1989**, *95*, 51–54. (b) Bersuker, I. B. *Chem. Rev.* **2001**, *101*, 1067–1114.

(19) (a) Evans, J. S. O.; Mary, T. A.; Vogt, T.; Subramanian, M. A.; Sleight, A. W. *Chem. Mater.* **1996**, *8*, 2809–2823. (b) Evans, J. S. O. *J. Chem. Soc., Dalton Trans.* **1999**, 3317–3326. (c) Ernst, G.; Broholm, C.; Kowach, G. R.; Ramirez, A. P. *Nature* **1998**, *396*, 147–149.

(20) Sastre, G.; Lewis, D. W. *J. Chem., Faraday Trans.* **1998**, *94*, 3049–3058.

(21) Shah, R.; Gale, J. D.; Payne, M. C. *Chem. Commun.* **1997**, 131–132.

(22) Ugliengo, P.; Civalleri, B.; Zicovich-Wilson, C. M.; Dovesi, R. *Chem. Phys. Lett.* **2000**, *318*, 247–255.

(23) Klima, S.; Thewalt, U. *J. Organomet. Chem.* **1988**, *354*, 77–81.

Table 1. Crystallographic Data for 2

empirical formula	C ₇₄ H ₁₀₆ O ₁₃ Zr ₆ ^a
fw	1750.91
color	colorless
cryst syst	monoclinic
space group	C2/m
a, Å	19.530(4)
b, Å	17.214(3)
c, Å	12.985(3)
β, deg	123.13(3)
V, Å ³	3655.9(13)
Z	2
ρ _{calc} , g cm ⁻³	1.591
μ, mm ⁻¹	0.884
F(000)	1788
2θ range, deg	3.44–49.42
no. of collected reflns	11 334
no. of unique reflns	3222 (R _{int} = 0.0502)
no. of data/restraints/params	3222/62/225
refinement method	full-matrix least-squares on F ²
R ^b wR2 ^c (I > 2σ(I))	0.0305, 0.0831
R, wR2 (all data), w;	0.0356, 0.0848
goodness of fit, S ^d	1.090
largest diff peak, hole (e Å ⁻³)	+0.611/−0.499

^a Including two toluene molecules; the eight hydrogen atoms of the hydroxide groups cannot be determined by X-ray diffraction. ^b $R = \sum ||F_o|| - ||F_c|| / \sum ||F_o||$. ^c $wR2 = [\sum w(F_o^2 - F_c^2)^2 / \sum w(F_o^2)]^{1/2}$. ^d $S = [\sum w(F_o^2 - F_c^2)^2 / \sum (n - p)]^{1/2}$.

of an isotopic distribution is tabulated. IR spectra were recorded on a Bio-Rad FTS-7 spectrometer as a Nujol mull between KBr plates. Elemental analyses were performed at the Analytical Laboratory of the Institute of Inorganic Chemistry, University of Göttingen.

[(Cp*Zr)₆(μ₄-O)(μ-O)₄(μ-OH)₈]₂(C₇H₈) (2). Ammonia (40 mL) was condensed onto the suspension of Cp*ZrCl₃ (0.665 g, 2.0 mmol) and KOH (KOH > 85%, H₂O 10–15%; 0.20 g, 3.0 mmol) in toluene (80 mL) at −78 °C with stirring. The stirring of the mixture was continued for 1 h at this temperature. Then the excess of ammonia was allowed to evaporate from the reaction mixture over a period of 4 h. During this time the mixture slowly warmed to room temperature. After filtration, the resulting colorless solution was kept at room temperature for four weeks to isolate colorless crystals of **2** (0.12 g, 20%). Mp > 410 °C. IR (Nujol): 3689 m, 1654 bm, 1306 s, 1261 m, 1093 s, 1022 s, 799 s, 730 s, 657 m, 610 m, 535 m (cm⁻¹). ¹H NMR (200 MHz, C₆D₆): δ 2.05 (C₅Me₅). EI-MS: *m/z* (%) 1512 (18) [M − C₇H₈ − Cp* − H₂O − H]⁺, 1367 (56) [M − 2 C₇H₈ − Cp* − 4 H₂O]⁺, 119 (100) [Cp* − CH₄]⁺. Anal. Calcd for C₇₄H₁₁₄O₁₃Zr₆ (1759.0): C, 50.5; H, 6.5; Zr, 31.1. Found: C, 50.1; H, 6.5; Zr, 31.1.

X-ray Analysis of 2. Single crystals of **2**, suitable for X-ray structural analysis, were obtained from toluene by keeping the

Table 2. Selected Bond Lengths (Å) and Bond Angles (deg) for [(Cp*Zr)₆(μ₄-O)(μ-O)₄(μ-OH)₈]₂(C₇H₈) (2)

Bond Lengths			
Zr(1)–O(1)	2.292(4)	Zr(1)–O(2)	2.171(2)
Zr(1)–O(3)	2.107(2)	Zr(1)–O(4)	2.072(2)
Zr(1)–O(5)	2.075(2)	Zr(2)–O(1)	2.610(10)
Zr(2)–O(1A) ^a	2.554(10)	Zr(2)–O(5)	2.081(2)
Zr(2)–O(3B) ^b	2.130(2)	Zr(2)–O(3C) ^c	2.130(2)
Zr(1B)···O(1)	2.966	Zr(1)···Zr(2)	3.608(1)
Zr(1)···Zr(1A)	3.564(1)	O(1)···O(1A)	0.933(13)
Bond Angles			
O(2)–Zr(1)–O(3)	82.76(6)	O(2)–Zr(1)–O(5)	83.39(6)
O(3)–Zr(1)–O(4)	88.35(9)	O(4)–Zr(1)–O(5)	88.94(10)
O(5)–Zr(2)–O(5A)	88.38(11)	O(5)–Zr(2)–O(3C)	85.93(8)
O(5A)–Zr(2)–O(3B)	85.93(8)	O(3B)–Zr(2)–O(3C)	85.20(11)
Zr(1)–O(3)–Zr(2A)	120.25(9)	Zr(1)–O(5)–Zr(2)	120.52(9)
Zr(1)–O(4)–Zr(1A)	118.70(14)	Zr(1)–O(2)–Zr(1C)	122.78(12)
Zr(1A)–Zr(1)–Zr(2)	60.401(12)		

^a A: *x*, −*y*, *z*. ^b B: −*x*, −*y*, −*z*. ^c C: −*x*, *y*, −*z*.

reaction mixture at room temperature for one month. Data for the structure were collected on a STOE IPDS II diffractometer. Intensity measurement was performed at 133(2) K on a rapidly cooled crystal in an oil drop²⁴ in the range 3.44° ≤ 2θ ≤ 49.42°. Of the 11 334 measured reflections, 3222 were independent (R_{int} = 0.0502). The structure was solved by direct methods (SHELXS-97)²⁵ and refined with all data by full-matrix least-squares on F² (SHELXL-97) (225 parameters). The hydrogen atoms of C–H bonds were placed in idealized positions. Other details of the data collection, structure solution, and refinement are listed in Table 1. Refinement in the acentric space group C2 leads to the same disorder in the center of the cluster. In C2/m Zr(2) is located on a mirror plane (position *j*), and Zr(1) is located on the position *j*.

Acknowledgment. This work was supported by the Deutsche Forschungsgemeinschaft, the Fonds der Chemischen Industrie, and the Göttinger Akademie der Wissenschaften.

Supporting Information Available: X-ray crystallographic data (excluding structure factors) for the structure **2** reported in this paper. This material is available free of charge via the Internet at <http://pubs.acs.org>.

OM0301132

(24) Clegg, W. *Acta Crystallogr.* **1981**, *A37*, 22–28.

(25) Sheldrick, G. M. *SHELX-97: Program for the Solution and Refinement of Crystal Structures*; Universität Göttingen: Göttingen, Germany, 1997.